China Ocean Engineering, Vol.22, No.3, pp.371 - 384

An Approximate Method for Calculation of Fluid Force and Response of A Circular Cylinder at Lock-in*

WANG Yi (王 艺)[1]

Division of Engineering Sciences, Institute of Mechanics, Chinese Academy of Sciences, Beijing 100190, China

(Received 26 August 2007; received revised form 30 April 2008; accepted 10 June 2008)

ABSTRACT

In this paper, equations calculating lift force of a rigid circular cylinder at lock-in in uniform flow are deduced in detail. Besides, equations calculating the lift force on a long flexible circular cylinder at lock-in are deduced based on mode analysis of a multi-degree freedom system. The simplified forms of these equations are also given. Furthermore, an approximate method to predict the forces and response of rigid circular cylinders and long flexible circular cylinders at lock-in is introduced in the case of low mass-damping ratio. A method to eliminate one deficiency of these equations is introduced. Comparison with experimental results shows the effectiveness of this approximate method.

Key words: *vortex-induced vibration*; *circular cylinder*; *lock-in*; *phase*; *lift*; *amplitude*

1. Introduction

Vortex-induced vibration (VIV) of circular cylindrical structures in steady uniform flow is of practical interest to deep-sea exploitation and other fields of engineering. The need to understand VIV has lead to a large number of fundamental studies. Feng (1968) used a flexible cylinder with one degree of freedom in a wind tunnel to investigate cross-flow vibration at a relatively large mass-damping ratio (the product of mass ratio and damping ratio) 0.255 and Reynolds numbers between 1.0×10^4 and 5×10^4. Brika and Laneville (1993) performed a series of thorough experiments in a wind tunnel with a flexible circular tube allowed to vibrate only in the transverse direction in a range of relatively low Reynolds number from 3.4×10^3 to 1.18×10^4 and at mass-damping ratios from 0.170482 for small amplitudes to 0.4108 for larger amplitudes. At lower mass-damping ratios smaller than 0.05, Khalak and Williamson (1996, 1997a, 1997b, 1999) performed a series of experiments in a water channel to study VIV of rigid cylinders. Some important phenomena such as bifurcations, two amplitude branches of resonance (Feng, 1968; Brika and Laneville, 1993) at high mass-damping ratio and three amplitude branches of resonance (Khalak and Williamson, 1996, 1997a, 1997b, 1999) at low mass-damping ratio, jump from one branch to another, abrupt change of phase, different vortex shedding modes, hysteresis loop, intermittently switching mode were observed.

* This work is financially supported by the National High Technology Research and Development Program of China (863 Program, Grant Nos. 2006AA09Z301 and 2006AA09A103-4), the National Natural Science Foundation of China (Grant No. 10532070) and the Knowledge Innovation Program of the Chinese Academy of Sciences (Grant No. KJCX2-YW-L02)

1 Corresponding author. E-mail: wangyimailbox@yeah.net

On the basis of experimental observations, Sarpkaya (1979) and Bearman (1984) showed that for a rigid cylinder constrained to move in the transverse direction the displacement and lift force at lock-in can be approximated by a sinusoidal function with a phase angle φ. From above approximation, several important relations are found through linear theoretical analysis (Khalak and Williamson, 1996; Govardhan and Williamson, 2000). However, the equations describing these relations have not been verified with experimental results.

In this paper, these equations are deduced in detail and simplified forms of these equations are also given in the case of low mass-damping ratio. Equations used to calculate phase are also given. Furthermore, an approximate method to predict the response and fluid force of rigid circular cylinders and long flexible circular cylinders at lock-in in uniform flow is introduced in the case of low mass-damping ratio. A method to eliminate one deficiency of these equations is introduced. Comparison with experimental results shows the effectiveness of this approximate method and these equations.

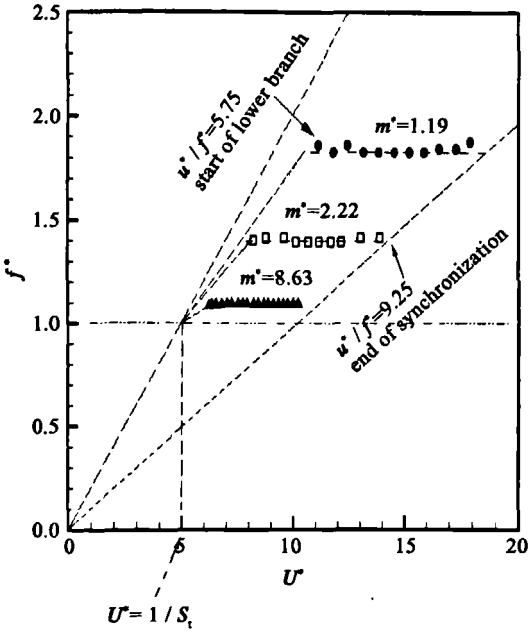

Fig. 1. The relationship among f^*, U^* and U^* in the lock-in range when ($m^*\zeta$) is very low. m^* is mass ratio; ζ is damping ratio; St is the Strouhal number; horizontal lines represent the lower branch. (Govardhan and Williamson, 2000).

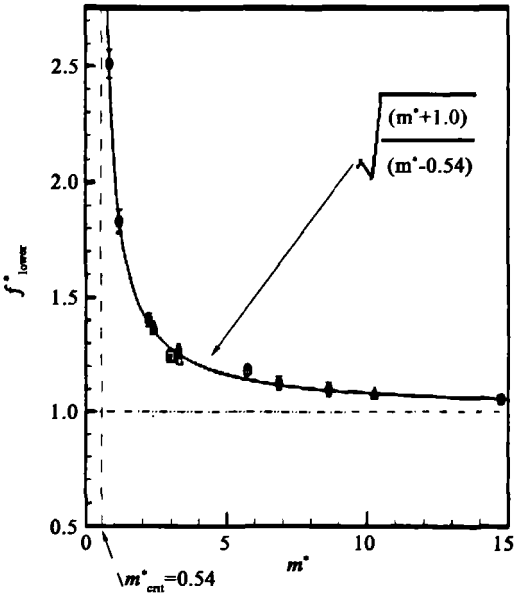

Fig. 2. Frequency versus mass ratio of a circular cylinder undergoing VIV at the lower branch. ● Govardhan (2000) △ Khalak (1999) □ Hover (1998) ⊙ Anand (1985) (Govardhan and Williamson, 2000).

2. Frequency

According to experimental results in the case of low mass-damping ratio, Govardhan and

Williamson (2000) gave the relationship between frequency ratio and reduced velocity for circular cylinders at lock-in in Figs. 1 and 2. The following information can be obtained from Figs. 1 and 2:

(1) Mass ratio $m^* < 10.0$

$$f^* = U^*/5.75, \quad \text{when} \quad 5.75f^*_{\text{lower}} > U^* \geq 1/St \tag{1}$$

$$f^* = f^*_{\text{lower}} = \sqrt{\frac{m^* + 1.0}{m^* - 0.54}}, \quad \text{when} \quad 9.25f^*_{\text{lower}} > U^* \geq 5.75f^*_{\text{lower}} \tag{2}$$

where reduced velocity $U^* = U/(f_{n0}D)$, mass ratio $m^* = m/m_D$ and frequency ratio $f^* = f/f_{n0} = \sqrt{\frac{m + m_D}{m + m_a}}$, m is the mass of the cylinder; m_D is the displaced mass of fluid; m_a is the added mass; f is the frequency of a circular cylinder at lock-in; f_{n0} is the natural frequency of a cylinder in still water and $f_{n0} = \frac{1}{2\pi}\sqrt{k/(m + m_D)}$; k is the linear spring constant; St is the relevant Strouhal number when lock-in starts and $St = f_{st}D/U$; f_{st} is the vortex shedding frequency of a body at rest; U is inflow velocity; D is the diameter of the cylinder.

(2) Mass ratio $m^* \geqslant 10.0$

When $m^* = 10.0$, the cylinder almost directly turns into the lower branch as soon as lock-in or synchronization starts and $f^* = f^*_{\text{lower}} \approx 1.0$, i.e.

$$f^* = f^*_{\text{lower}} = \sqrt{\frac{m^* + 1.0}{m^* - 0.54}}, \quad \text{when} \quad 9.25f^*_{\text{lower}} > U^* > 1/St. \tag{3}$$

3. Added Mass

Sarpkaya (1978, 2004) and Vikestad *et al.* (2000) pointed out that the added mass m_a is not equal to the ideal added mass and can change from positive to negative in the whole lock-in range of VIV. Wang *et al.* (2007) gave the following estimation formulas of added mass coefficient for a circular cylinder at lock-in.

3.1 Mass Ratio $m^* < 10.0$

When $5.75f^*_{\text{lower}} > U^* > 5.0$, the added mass coefficient $C_a = m_a/m_D$ can be obtained:

$$C_a = \frac{m^* + 1}{G^2} - m^* \quad \text{when} \quad 5.75f^*_{\text{lower}} > U^* > 1/St \tag{4}$$

where $G = \frac{f^*_{\text{lower}} - 1.0}{5.75f^*_{\text{lower}} - 1/St}(U^* - 5.0) + 1.0$. Strouhal number St is close to 0.2 when $100000 > Re > 200$ (Roshko, 1954; Fernando and Hassan, 2005).

When $9.25f^*_{\text{lower}} > U^* \geqslant 5.75f^*_{\text{lower}}$, because $f^* = f^*_{\text{lower}}$, i.e. $\sqrt{\frac{m + m_D}{m + m_a}} = \sqrt{\frac{m^* + 1.0}{m^* - 0.54}}$. The added mass coefficient is

$$C_a = -0.54, \quad \text{when} \quad 9.25f^*_{\text{lower}} > U^* \geq 5.75f^*_{\text{lower}} \tag{5}$$

3.2 Mass Ratio $m^* \geqslant 10.0$

$$C_a = -0.54, \text{ when} \quad 9.25f^*_{\text{lower}} > U^* > 1/St \tag{6}$$

Eqs. (4) ~ (6) are the semi-empirical formulas for the added mass of a circular cylinder at lock-in.

4. Transverse Force

4.1 Single-Degree-of-Freedom

A spring-mass-damping model shown in Fig. 3 is adopted to study a circular cylinder at lock-in. The equation of motion is

$$m\ddot{y} + c\dot{y} + ky = F_Y(t)$$

$F_Y(t)$ is the lift force of fluid and y is the displacement of the cylinder.

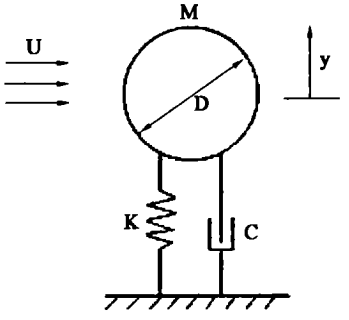

Fig. 3. Spring-mass-damping model.

Above equation can be changed into another form:

$$m\{\ddot{y} + 2\zeta_0\omega_0\dot{y} + \omega_0^2 y\} = F_Y(t), \tag{7}$$

where $\omega_0 = \sqrt{\frac{k}{m}}$, damping ratio $\zeta_0 = \frac{c}{2\sqrt{km}}$.

At lock-in, a good approximation to the displacement and lift force (Sarpkaya, 1979; Bearman, 1984) is

$$y = A\sin\omega t, \quad F_Y(t) = \bar{F}_Y\sin(\omega t + \phi), \tag{8}$$

where $\omega = 2\pi f$.

Substituting $F_Y(t) = \bar{F}_Y[\sin\omega t\cos\phi + \cos\omega t\sin\phi]$ into Eq. (7), one can obtain:

$$m\{\ddot{y} + 2\zeta_0\omega_0\dot{y} + \omega_0^2 y\} = \bar{F}_Y[\sin\omega t\cos\phi + \cos\omega t\sin\phi].$$

According to Eq. (8), $\sin\omega t = -\frac{\ddot{y}}{A\omega^2}$ and $\cos\omega t = \frac{\dot{y}}{A\omega}$. The lift force of fluid may be split into two components. One in phase with the cylinder acceleration is $-\frac{\bar{F}_Y\cos\phi}{A\omega^2}\ddot{y}$ and the other in phase with velocity is $\frac{\bar{F}_Y\sin\phi}{A\omega}\dot{y}$ (Vikestad *et al.*, 2000). Eq. (7) then becomes

$$m\{\ddot{y} + 2\zeta_0\omega_0\dot{y} + \omega_0^2 y\} = -\frac{\bar{F}_Y\cos\phi}{A\omega^2}\ddot{y} + \frac{\bar{F}_Y\sin\phi}{A\omega}\dot{y}.$$

Above equation can also be changed into

$$[m + \frac{\bar{F}_Y \cos\phi}{A\omega^2}]\ddot{y} + 2m\zeta_0\omega_0\dot{y} + m\omega_0^2 y = \frac{\bar{F}_Y \sin\phi}{A\omega}\dot{y}.$$

According to the definition of added mass, the expression of added mass is $m_a = \frac{\bar{F}_Y \cos\phi}{A\omega^2}$ (Willden and Graham, 2001). Above equation can be changed into another form

$$(m + m_a)\ddot{y} + 2m\zeta_0\omega_0\dot{y} + m\omega_0^2 y = \frac{\bar{F}_Y \sin\phi}{A\omega}\dot{y}. \tag{9}$$

Substituting $y = A\sin\omega t$ into Eq. (9). Equating sine and cosine terms, one can obtain

$$-(m + m_a)\omega^2 + m\omega_0^2 = 0, \tag{10}$$

$$2\zeta_0\omega_0 m = \frac{\bar{F}_Y \sin\phi}{A\omega}. \tag{11}$$

In addition,

$$m_a = \frac{\bar{F}_Y \cos\phi}{A\omega^2}. \tag{12}$$

In the case of $m_a \neq 0$, $\tan\phi = \frac{2m\zeta_0\omega_0}{m_a\omega}$ can be obtained from Eqs. (11) and (12), i.e.

$$\phi = \begin{cases} \arctan\left(\frac{2m^*\zeta_0 f_0^*}{C_a f^*}\right), & \text{when } C_a > 0 \\ \pi + \arctan\left(\frac{2m^*\zeta_0 f_0^*}{C_a f^*}\right), & \text{when } C_a < 0 \end{cases}$$

$$= \begin{cases} \arctan\left(\frac{2\zeta\sqrt{m^* + C_a}\sqrt{m^* + C_A}}{C_a}\right), & \text{when } C_a > 0 \\ \pi + \arctan\left(\frac{2\zeta\sqrt{m^* + C_a}\sqrt{m^* + C_A}}{C_a}\right), & \text{when } C_a < 0 \end{cases} \tag{13}$$

in which, $\zeta = \frac{c}{2\sqrt{k(m + m_A)}} = \zeta_0\sqrt{\frac{m^*}{m^* + C_A}}$. m_A is ideal added mass, $C_A = \frac{m_A}{m_D}$ is ideal added mass coefficient, and $C_A = 1.0$ for a circular cylinder.

In addition, from Eq. (11) the relation between lift and amplitude can be deduced:

$$\bar{F}_Y = \frac{2m\omega\omega_0\zeta_0}{\sin\phi}A,$$

or written in another form:

$$\bar{C}_Y = \frac{4\pi^3 m^*\zeta_0 f^* f_0^*}{U^{*2}\sin\phi}A^*,$$

where $\bar{C}_Y = \frac{\bar{F}_Y}{\frac{1}{2}\rho U^2 D}$, ρ being the density of fluid.

Substituting $\zeta_0 = \zeta\sqrt{\frac{m^* + C_A}{m^*}}$ and $f_0^* = \sqrt{\frac{m^* + C_A}{m^*}}$ into above equation leads to:

$$\bar{C}_Y = \frac{4\pi^3(m^* + C_A)\zeta f^*}{U^{*2}\sin\phi}A^* \tag{14}$$

This is the equation given by Khalak and Williamson (1996, 1999, 2004) for a rigid circular cylinder at lock-in. However, they do not give any detail of deduction.

At lock-in, experiments show that the amplitude of lift coefficient $\bar{C}_Y$ and the amplitude of vibration A^* are time-dependent (Morse and Williamson, 2006). Sometimes $\bar{C}_Y$ is substituted with $\bar{C}_{Y\mathrm{rms}}(t)$ and A^* is substituted with $A^*_{\mathrm{rms}}(t)$, where subscript 'rms' means root mean square value. Then Eq. (14) can be written in another form:

$$\bar{C}_{Y\mathrm{rms}}(t) = \frac{4\pi^3(m^* + C_A)\zeta f^*}{U^{*2}\sin\phi} A^*_{\mathrm{rms}}(t). \tag{15}$$

Because $\bar{C}_Y = \sqrt{2}C_Y(t)_{\mathrm{rms}}$ and $A^* = \sqrt{2}y^*_{\mathrm{rms}}$, the following equations can be obtained from Eq. (14):

$$C_{Y\mathrm{rms}} = \frac{2\sqrt{2}\pi^3(m^* + C_A)\zeta f^*}{U^{*2}\sin\phi} A^* \tag{16}$$

or

$$C_{Y\mathrm{rms}} = \frac{4\pi^3(m^* + C_A)\zeta f^*}{U^{*2}\sin\phi} y^*_{\mathrm{rms}}. \tag{17}$$

Because $\sin\phi \approx \tan\phi$ in the case of low $m^*\zeta$, $\sin\phi \approx \dfrac{2\zeta\sqrt{m^* + C_a}\sqrt{m^* + C_A}}{|C_a|}$ can be obtained from Eq. (13). Substitute it into Eq. (16), and then the simplified form of Eq. (16) is

$$C_{Y\mathrm{rms}} = \frac{\sqrt{2}\pi^3\sqrt{m^* + C_A}\,|C_a|\,f^*}{U^{*2}\sqrt{m^* + C_a}} A^*. \tag{18}$$

4.2 Application to A Long Flexible Circular Cylinder at Lock-in

A long flexible circular cylinder can be analyzed with finite element method. Experiment (Brika and Laneville, 1993) showed that variation of phase ϕ along a long flexible circular cylinder at lock-in is very small. Therefore, every element of the long flexible circular cylinder can be considered to be under single-degree-freedom VIV with the same phase ϕ and not affected by the variation of the vibration amplitude along the long flexible circular cylinder. From Eqs. (14) and (16) one can deduce that the lift force along a long flexible circular cylinder is in direct proportion to the amplitude along a long flexible circular cylinder.

Since the lift along a long flexible circular cylinder has a mode similar to the amplitude along a long flexible circular cylinder in uniform flow, which is also shown by Evangelinos *et al*. (2000), linear theory can also be applied to a long flexible circular cylinder at lock-in. At lock-in, vortex shedding frequency is equal to the natural frequency of a long flexible circular cylinder with added mass taken into consideration. $\boldsymbol{\Phi}$ is mode shape vector and the element which reflects the largest amplitude along the circular cylinder should be 1.0. For example, the middle element of the 1st mode shape vector $\boldsymbol{\Phi}$ should be 1.0 for a long flexible circular cylinder with two simply supported ends. The first or the last element of the 1st mode shape vector $\boldsymbol{\Phi}$ should be 1.0 for a long flexible circular cylinder with only one built-in end.

The equation of a long flexible circular cylinder undergoing linear vibration is

$$\{M\}\ddot{X} + \{C\}\dot{X} + \{K\}X = \{f_L(t)\}$$

where $X = \Phi A\sin(\omega t)$. A is the largest amplitude along the cylinder, $\{M\}$ is mass matrix, $\{C\}$ is damp matrix, and $\{K\}$ is stiffness matrix.

Assume the lift $\{f_L(t)\} = \{F_L\}\sin(\omega t + \phi)$,

$$\{M\}\ddot{X} + \{C\}\dot{X} + \{K\}X = \{F_L\}\sin(\omega t + \phi)$$

i.e. $$\{M\}\ddot{X} + \{C\}\dot{X} + \{K\}X = \{F_L\}\sin(\omega t)\cos\phi + \{F_L\}\cos(\omega t)\sin\phi.$$

As $\sin(\omega t) = -\Phi^{\mathrm{T}}\ddot{X}/(\Phi^{\mathrm{T}}\Phi A\omega^2)$ can be obtained from $X = \Phi A\sin(\omega t)$, the following equation

$$\left(\{M\} + \frac{\{F_L\}\Phi^{\mathrm{T}}}{\Phi^{\mathrm{T}}\Phi A\omega^2}\cos\phi\right)\ddot{X} + \{C\}\dot{X} + \{K\}X = \{F_L\}\cos(\omega t)\sin\phi$$

can be obtained.

According to the definition of added mass, added mass matrix is

$$\{M_a\} = \frac{\{F_L\}\Phi^{\mathrm{T}}}{\Phi^{\mathrm{T}}\Phi A\omega^2}\cos\phi,$$

then $$(\{M\} + \{M_a\})\ddot{X} + \{C\}\dot{X} + \{K\}X = \{F_L\}\cos(\omega t)\sin\phi.$$

Substituting $X = \Phi A\sin(\omega t)$ into above equation and equating sine and cosine terms, one can obtain

$$[-(\{M\} + \{M_a\})\omega^2 + \omega_0^2\{M\}]\Phi = 0$$

$$\{C\}\Phi A\omega = \{F_L\}\sin\phi$$

where ω_0 is the 1st natural angular frequency.

In addition, $$\{M_a\} = \frac{\{F_L\}\Phi^{\mathrm{T}}}{\Phi^{\mathrm{T}}\Phi A\omega^2}\cos\phi.$$

From above two equations, the following two equations can be obtained:

$$\Phi^{\mathrm{T}}\{C\}\Phi A\omega = \Phi^{\mathrm{T}}\{F_L\}\sin\phi;$$

$$\Phi^{\mathrm{T}}\{M_a\}\Phi A\omega^2 = \Phi^{\mathrm{T}}\{F_L\}\cos\phi.$$

From the above equations one can obtain

$$\tan\phi = \frac{\Phi^{\mathrm{T}}\{C\}\Phi}{\Phi^{\mathrm{T}}\{M_a\}\Phi\omega} = \frac{2m^*\Phi^{\mathrm{T}}\{\zeta_0\}\Phi f_0^*}{\Phi^{\mathrm{T}}\{C_a\}\Phi f^*}.$$

So,

$$\phi = \begin{cases} \arctan\left(\dfrac{2m^*\Phi^{\mathrm{T}}\{\zeta_0\}\Phi f_0^*}{\Phi^{\mathrm{T}}\{C_a\}\Phi f^*}\right), & \text{when } C_a > 0 \\ \pi + \arctan\left(\dfrac{2m^*\Phi^{\mathrm{T}}\{\zeta_0\}\Phi f_0^*}{\Phi^{\mathrm{T}}\{C_a\}\Phi f^*}\right), & \text{when } C_a < 0 \end{cases}$$

$$= \begin{cases} \arctan\left(\dfrac{2\Phi^{\mathrm{T}}\{\zeta\}\Phi\sqrt{m^* + C_A}\sqrt{m^* + C_a}}{\Phi^{\mathrm{T}}\{C_a\}\Phi}\right), & \text{when } C_a > 0 \\ \pi + \arctan\left(\dfrac{2\Phi^{\mathrm{T}}\{\zeta\}\Phi\sqrt{m^* + C_A}\sqrt{m^* + C_a}}{\Phi^{\mathrm{T}}\{C_a\}\Phi}\right), & \text{when } C_a < 0 \end{cases}$$

where $\{C_a\} = C_a\{I\}$ is a diagonal matrix of added mass, $\{\zeta\} = \zeta\{I\}$ is the diagonal matrix of damping ratio. Above equation turns into

$$\phi = \begin{cases} \arctan\left(\dfrac{2\zeta\sqrt{m^* + C_a}\sqrt{m^* + C_A}}{C_a}\right), & \text{when} \quad C_a > 0 \\ \pi + \arctan\left(\dfrac{2\zeta\sqrt{m^* + C_a}\sqrt{m^* + C_A}}{C_a}\right), & \text{when} \quad C_a < 0 \end{cases} \tag{19}$$

which is the same as Eq. (13).

In addition $\{F_L\} = \dfrac{\{C\}\boldsymbol{\Phi}A\omega}{\sin\phi}$,

then the amplitude of lift coefficient is

$$\{\bar{C}_L\} = \frac{\{C\}\boldsymbol{\Phi}A\omega}{\sin\phi\,\frac{1}{2}\rho U^2 Dl} = \frac{2\{C\}\boldsymbol{\Phi}A\omega\,\frac{1}{4}\pi D^2}{\sin\phi\rho U^2 Dl\,\frac{1}{4}\pi D^2} = \frac{2\{C\}\boldsymbol{\Phi}A\omega\,\frac{1}{4}\pi D^2}{\sin\phi U^2 Dm_{Dl}}$$

$$= \frac{2\{C\}\boldsymbol{\Phi}A\omega\,\frac{1}{4}\pi D^2}{\sin\phi U^2 D}\frac{m_l}{m_{Dl}}\frac{1}{m_l} = \frac{\{C\}\boldsymbol{\Phi}Af\pi^2 D}{\sin\phi U^2}m^*\frac{1}{m_l} = \frac{2\{\zeta_0\}\omega_0\boldsymbol{\Phi}Af\pi^2 D^2}{\sin\phi U^2 D}m^*$$

$$= \frac{2\{\zeta_0\}\omega_0\boldsymbol{\Phi}Af\pi^2 D^2}{\sin\phi U^{*2}f_{n0}^2 D^3}m^* = \frac{2\{\zeta_0\}\omega_0\boldsymbol{\Phi}f\pi^2 m^* A^*}{\sin\phi U^{*2}f_{n0}^2} = \frac{4\pi^3\{\zeta_0\}\boldsymbol{\Phi}f_0 f m^* A^*}{\sin\phi U^{*2}f_{n0}^2}$$

$$= \frac{4\pi^3 m^*\{\zeta_0\}\boldsymbol{\Phi}f_0^* f^*}{U^{*2}\sin\phi}A^*,$$

where l is the length of a finite element, m_{Dl} is the displaced fluid mass of a finite element, damping ratio matrix $\{\zeta_0\} = \{C\}/(2m_l\omega_0)$ and m_l is the mass of a finite element.

Thus, the root mean square of lift coefficient along the long flexible circular cylinder is

$$\{C_{Lrms}\} = \frac{2\sqrt{2}\pi^3 m^*\{\zeta_0\}\boldsymbol{\Phi}f_0^* f^*}{U^{*2}\sin\phi}A^*.$$

Substituting $\{\zeta_0\} = \{\zeta\}\sqrt{\dfrac{m^* + C_A}{m^*}}$ and $f_0^* = \sqrt{\dfrac{m^* + C_A}{m^*}}$ into above equation leads to

$$\{C_{Lrms}\} = \frac{2\sqrt{2}\pi^3(m^* + C_A)\{\zeta\}\boldsymbol{\Phi}f^*}{U^{*2}\sin\phi}A^*. \tag{20}$$

The lift distribution along a long flexible circular cylinder can be worked out with Eq. (20).

Since $\sin\phi \approx \tan\phi$ in the case of low $m^*\zeta$, $\sin\phi \approx \dfrac{2\zeta\sqrt{m^* + C_A}\sqrt{m^* + C_a}}{|C_a|}$ can be obtained from Eq. (19). Substituting it into Eq. (20), one can obtain the simplified form of Eq. (20):

$$\{C_{Lrms}\} = \frac{\sqrt{2}\pi^3\sqrt{m^* + C_A}\,|C_a|\,f^*}{U^{*2}\sqrt{m^* + C_a}}A^*\boldsymbol{\Phi}, \tag{21}$$

which is similar to Eq. (18).

4.3 Dynamical Instability Area

When $m^* \geqslant 10.0$, a circular cylinder can be approximately considered to be in the lower branch as soon as lock-in or synchronization starts and added mass coefficient is $C_a = -0.54$.

When $m^* < 10.0$, added mass may turn from positive into negative. From Eq. (4) one can obtain added mass coefficient $C_a = 0$ when reduced velocity is

$$U_T^* = \frac{5.75 f_{\text{lower}}^* - 5.0}{f_{\text{lower}}^* - 1.0}\left(\sqrt{\frac{m^* + 1}{m^*}} - 1.0\right) + 5.0 \tag{22}$$

Phase jump and amplitude jump between upper branch and lower branch also occurs when reduced velocity U^* is equal to U_T^* (Williamson and Govardhan, 2004). This is roughly shown in Fig. 4.

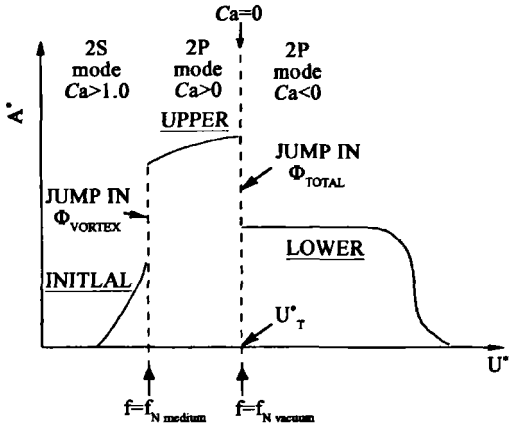

Fig. 4. Overview diagram of the low-$m^* \zeta$ type of response.

The amplitude and phase do not have one value in the intermittent switching region from upper branch to lower branch (Morse and Williamson, 2006), which is shown in Fig. 5. So, the switching region where C_a is close to zero is a dynamical instability area.

When $m^* \zeta$ is in a small quantity, it can be concluded from Eq. (11) that $\sin \phi$ should also be in a small quantity. So $|\cos \phi| \approx 1.0$ can also be obtained. When added mass $m_a \approx 0$, $|\cos \phi|$ is close to zero according to Eq. (12). Thus, Eqs. (11) and (12) conflict with each other when $C_a \approx 0$. Linear theory is no longer valid in this region. This is the reason that Eqs. (11) and (12) conflict with each other when $C_a \approx 0$. Eqs. (13) ~ (18) and Eqs. (19) ~ (21) are no longer valid in this region either.

Since $C_a \approx 0$ appears at lock-in only when $m^* < 10.0$, dynamic instability area appears only under the condition $m^* < 10.0$. When $m^* \geqslant 10.0$, the influence of dynamic instability area can be neglected.

5. Amplitude

From the Griffin plot for the circular cylinder only in transverse VIV (Griffin, 1980; Khalak and

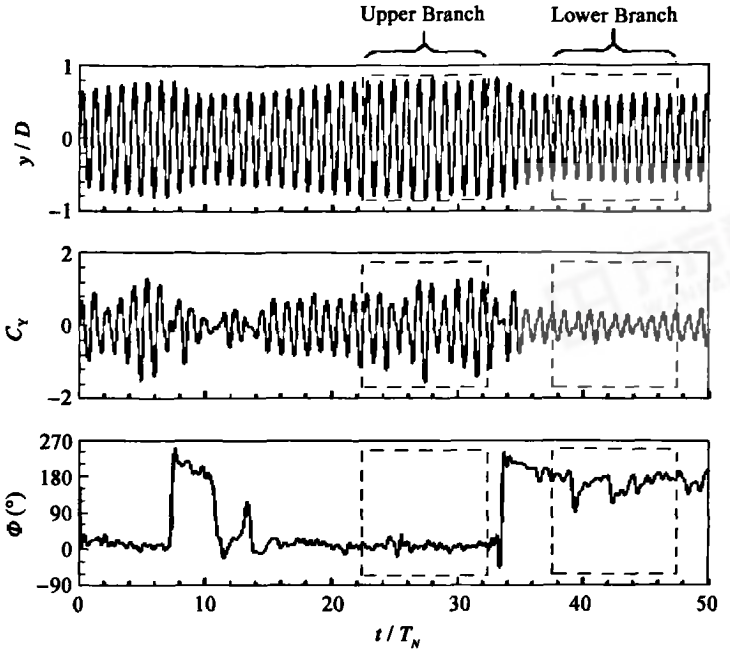

Fig. 5. Amplitude, lift and phase in the intermittent switching region from upper branch to lower branch, where $T_N = 1/f_{n0}$ (Morse and Williamson, 2006).

Williamson, 1999; Govardhan and Williamson, 2000), the following empirical formulas can be obtained under the condition $(m^* + C_A)\zeta < 0.05$:

1. At the lower branch

$$A^* \approx 0.6, \tag{23}$$

2. At the upper branch

$$A^* \approx -0.3865 - 0.705\lg[(m^* + C_A)\zeta], \tag{24}$$

where $A^* = A/D$, A being the amplitude of the cylinder. Strictly, Eqs. (23) and (24) can be applied only to the peak amplitude, not the amplitude everywhere in the upper branch or the lower branch. However, Eqs. (23) and (24) can be used as an good approximation because of the small fluctuation of amplitude in the upper branch and the lower branch in the case of $(m^* + C_A)\zeta < 0.05$ (Govardhan and Williamson, 2000).

6. Approximate Method

An approximate method for a circular cylinder with low mass-damping ratio at lock-in in uniform flow is as follows:

Step 1. Calculate frequency ratio f^* at lock-in with Eqs. (1) ~ (3).

Step 2. Calculate added mass C_a at lock-in with Eqs. (4) ~ (6).

Step 3. Calculate amplitude at A^* lower branch and upper branch with Eqs. (23) ~ (24). The

amplitude of upper branch turns into the amplitude of lower branch at reduced velocity U_T^* which can be obtained from Eq. (22).

Step 4. Calculate phase ϕ according to Eq. (13) or Eq. (19).

Step 5. Calculate the root mean square of lift coefficient $C_{Y\text{rms}}$ according to Eqs. (16) and (20) or simplified Eqs. (18) and (21).

Step 6. Dispose of the deficiency of calculation in the dynamical instability area.

7. Comparison with Experimental Results of Rigid Circular Cylinders

7.1 Phase

(1) $m^* = 3.3$, $m^* \zeta = 0.00858$

Comparison with experimental results is shown in Fig. 6. Phase transition occurs at $U_T^* = 6.24$ according to Eq. (22).

(2) $m^* = 10.1$, $m^* \zeta = 0.0134$

Comparison with experimental results is shown in Fig. 7. The calculation shows that $\phi = 177.1°$ at $U^* = 5.84$ obtained from Eq. (13) is in good agreement with experimental results.

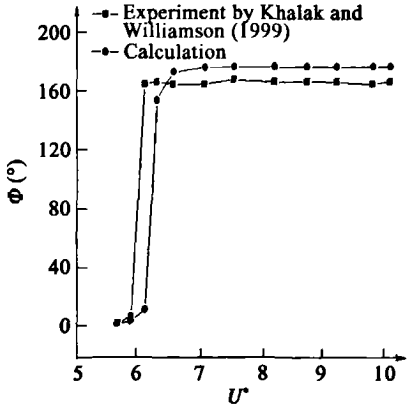

Fig. 6. $m^* = 3.3$, $m^* \zeta = 0.00858$.

7.2 Amplitude and Lift

When $m^* = 3.3$ and $m^* \zeta = 0.000858$, $A^* = 0.6$ at the lower branch and $A^* = 0.99$ at the upper branch can be obtained according to Eq. (23) and (24). When $m^* = 10.1$ and $m^* \zeta = 0.013534$, $A^* = 0.6$ at the lower branch can be obtained.

Comparisons among the calculated results given by Eq. (16), Eq. (18) and the experimental results given by Khalak and Williamson (1997a) are shown in Figs. 8 and 9. The results given by Eq. (16) and simplified Eq. (18) are close to each other, indicating that simplified Eq. (18) can also give good results in the case of low mass-damping ratio.

7.3 Disposal of the Deficiency

Fig. 8 shows that the difference between the calculated results and experimental results is large near the dynamical instability area mentioned in section 4.3. Since linear theory is no longer valid in

this region, Eqs. (13) ~ (18) and Eqs. (19) ~ (21) can only give wrong results in this region.

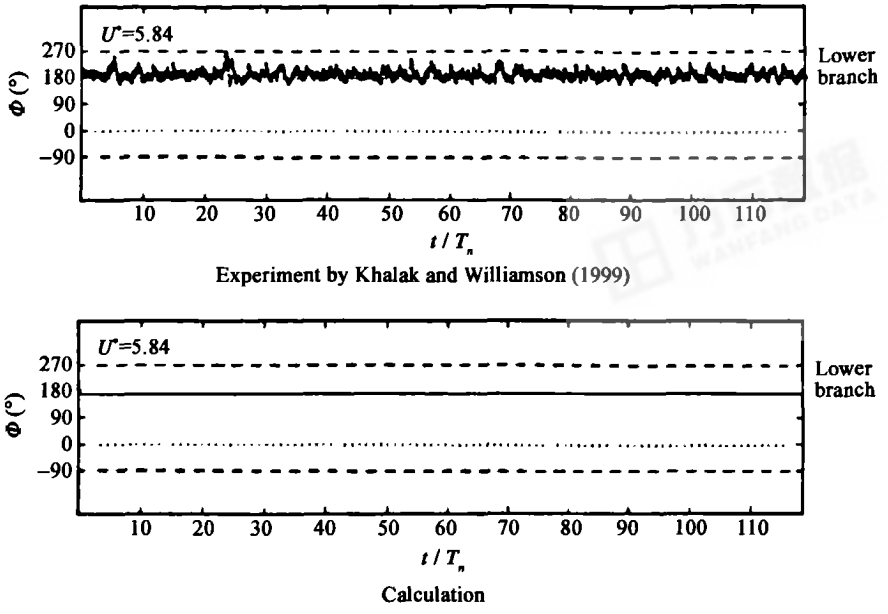

Fig. 7. $m^* = 10.1$, $m^*\zeta = 0.0134$.

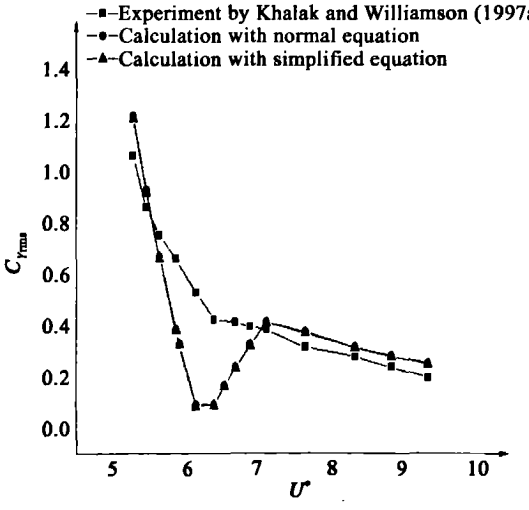

Fig. 8. $m^* = 3.3$, $m^*\zeta = 0.00858$.

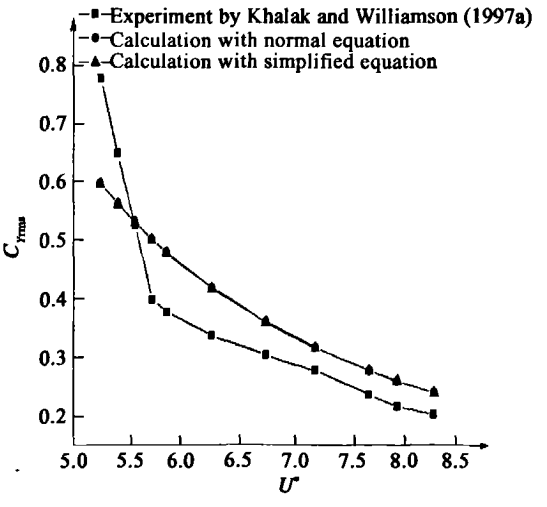

Fig. 9. $m^* = 10.1$, $m^*\zeta = 0.00134$.

The approaches to get rid of the deficiency are proposed as follows:

1. Calculate U_T^* according to Eq. (22) when $m^* < 10.0$.

2. Calculate $U_L^* = (1 - 5\%)\,U_T^*$ and $U_R^* = (1 + 5\%)\,U_T^*$

3. Phase between U_L^* and U_T^* is equal to the phase at U_L^*; phase between U_R^* and U_T^* is equal to the phase at U_R^*.

4. C^*_{Lrms} between U^*_L and U^*_R can be obtained through linear interpolation between C^*_{Lrms} at U^*_L and C^*_{Lrms} at U^*_R.

These approaches are shown in Figs. 10 and 11. If $m^* \geqslant 10.0$, there is no such deficiency.

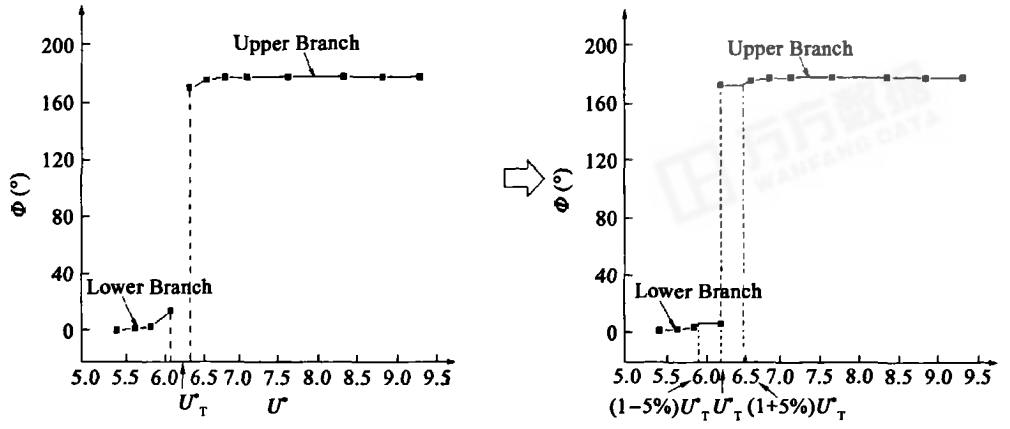

Fig. 10. Disposal to the discontinuous point of phase at lock-in.

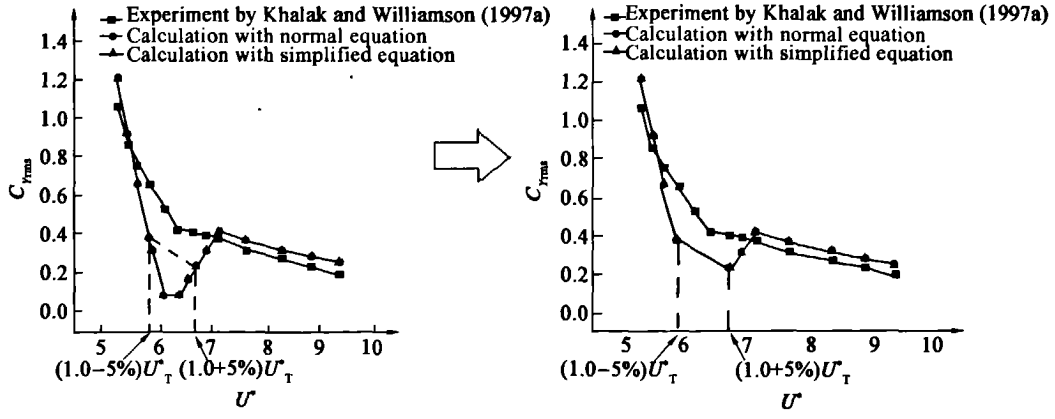

Fig. 11. Disposal to the deficiency of the lift at lock-in.

8. Discussions and Concluding Remarks

Through the linear theoretical analysis for a circular cylinder at lock-in, equations for calculating phase, lift coefficient of a rigid circular cylinder at lock-in are deduced in detail. Moreover, equations for calculating the phase and the lift distributed along a long flexible circular cylinder at lock-in can also be deduced through the linear mode analysis. Simplified forms of these equations are given too.

An approximate method to predict the response and fluid forces of rigid circular cylinders and flexible circular cylinders at lock-in in uniform flow is introduced in the case of low mass-damping ratio. One method to eliminate the deficiency in calculation is also given. Comparison with experimental results of rigid circular cylinders shows the effectiveness of this approximate method.

The preconditions for the equations and the approximate method are $m^* \geqslant 0.54$, $(m^* + C_A)\zeta$

< 0.05, $9.25 f^*_{\text{lower}} > U^* \geqslant 1/St$, and the circular cylinder only in transverse VIV.

Riser tubes and tension legs of deepwater platform at lock-in are mostly under nonlinear vibration when aspect ratios are not large enough. Strictly speaking, above approximate method and equations based on linear mode analysis of multi-DOF system can not be applied to them precisely. However, the approximate method given in this paper is an effective method in the case of large aspect ratio since there is no more other effective nonlinear theory used to analyse VIV of long flexible circular cylinders now.

References

Bearman, P. W., 1984. Vortex shedding from oscillating bluff bodies, *Annu. Rev. Fluid Mech.*, **16**, 195 ~ 222.

Brika, D. and Laneville, A., 1993. Vortex-induced vibrations of a long flexible circular cylinder, *J. Fluid Mech.*, **250**, 481 ~ 508.

Evangelinos, C., Lucor, D. and Karniadakis, G. E., 2000. DNS-derived force distribution on flexible cylinders subject to vortex-induced vibration, *J. Fluids Struct.*, **14**(3): 429 ~ 440.

Feng, C-C., 1968. *The measurement of vortex induced effects in flow past stationary and oscillating circular and d-section cylinders*, Master's Thesis, Department of Mechanical Engineering, The University of British Columbia, Canada.

Fernando, L. P. and Hassan, A., 2005. Vortex synchronization regions in shedding from an oscillating cylinder, *Physics of Fluids*, **17**(011703): 1 ~ 4.

Khalak, A. and Williamson, C. H. K., 1996. Dynamics of a hydroelastic cylinder with very low mass and damping, *J. Fluids Struct.*, **10**(5): 455 ~ 472.

Khalak, A. and Williamson, C. H. K., 1997a. Fluid forces and dynamics of a hydroelastic structure with very low mass and damping, *J. Fluids Struct.*, **11**(8): 973 ~ 982.

Khalak, A. and Williamson, C. H. K., 1997b. Investigation of relative effects of mass and damping in vortex-induced vibration of a circular cylinder, *Journal of Wind Engineering and Industrial Aerodynamics*, **69-71**, 341 ~ 350.

Khalak, A. and Williamson, C. H. K., 1999. Motions, forces and mode transitions in vortex-induced vibrations at low mass-damping, *J. Fluids Struct.*, **13**(7-8): 813 ~ 851.

Govardhan, R. and Williamson, C. H. K., 2000. Modes of vortex formation and frequency response of a freely vibrating cylinder, *J. Fluid Mech.*, **420**, 85 ~ 130.

Griffin, O. M., 1980. Vortex-excited cross-flow vibrations of a single cylindrical tube, *ASME J. Pressure Vessel Technol.*, **102**(2): 158 ~ 166.

Morse, T. L. and Williamson, C. H. K., 2006. Employing controlled vibrations to predict fluid forces on a cylinder undergoing vortex-induced vibration, *J. Fluids Struct.*, **22**(6-7): 877 ~ 884.

Roshko, A., 1954. On the development of turbulent wakes from vortex streets, NACA TR 1191

Sarpkaya, T., 1978. Fluid forces on oscillating cylinders, *Journal of Waterway Port Coastal and Ocean Divison*, ASCE, **104**, 275 ~ 290.

Sarpkaya, T., 1979. Vortex-induced oscillations, a selective review, *J. Appl. Mech.*, **46**(2): 241 ~ 258.

Sarpkaya, T., 2004. A critical review of the intrinsic nature of vortex-induced vibrations, *J. Fluids Struct.*, **19**(4): 389 ~ 447.

Vikestad, K., Vandiver, J. K. and Larsen, C. M., 2000. Added mass and oscillation frequency for a circular cylinder subjected to vortex-induced vibrations and external disturbance, *J. Fluids Struct.*, **14**(7): 1071 ~ 1088.

Wang Yi, Chen Weimin and Lin Mian, 2007. Variation of added mass and its application to the calculation of amplitude response for a circular cylinder, *China Ocean Eng.*, **21**(3): 429 ~ 437.

Willden, R. H. J. and Graham, J. M. R., 2001. Numerical prediction of VIV on long flexible circular cylinders, *J. Fluids Struct.*, **15**(3-4): 659 ~ 669.

Williamson, C. H. K. and Govardhan, R., 2004. Vortex-induced vibrations, *Annu. Rev. Fluid Mech.*, **36**, 413 ~ 455.